Industrial Engineering Journal
ISSN: 0970-2555
Volume : 53, Issue 4, No. 7, April : 2024

MCMT METHODOLOGY EMPLOYING FACIAL VEINS FOR INDIVIDUAL IDENTIFYING

Mohd Sahil M. Tech. Scholar of Department of computer Science, Rama University, Kanpur 209217, INDIA :mohdsahil570@gmail.com
Hari Om Sharan, Somendra Tripathi, C. S. Raghuvanshi Department of computer Science, Rama University, Kanpur 209217, INDIA
Email Id:deanacademicaffairs@ramauniversity.ac.in ;; drcsraghuvanshi.fet@ramauniversity.ac.in

Abstract:
Identifying individuals using the veins on their face is a difficult undertaking in the realm of identity and verification. The reason for this is that numerous additional methodologies fail to recognise the distinctiveness of an individual inside the universe. This study report explores the distinctiveness of an individual using a technology that analyses the veins in their face. This paper utilises five distinct individuals' facial vein photographs captured at various rotation angles, ranging from 900 to 2700 and 3150 degrees in both left and right directions. Each individual was represented by eight distinct photos, each taken at various rotations. From each of these images, the identical minimum cost minutiae tree (MCMT) was derived. In this context, either Prim's or Kruskal's approach is employed to determine the Minimum Cost Maximum Tree (MCMT) from a graph of minutiae. The MCMT is scanned in a pre-order manner to generate a string that consists of the vertices and the lengths of the edges, which is unique. For robustness testing, we adjusted the edge lengths of each MCMT by five pixels in both positive and negative directions. Our investigations have shown that the sequence of vertices and edge lengths of MCMT, which we refer to as the traversed string, is unique to each individual. This unique sequence has proven to accurately identify a person with an accuracy rate of 95%. In addition, we have conducted a performance comparison between our suggested technique and other established procedures. The results indicate that our suggested approach shows excellent results.
Keywords: Face Vein, Minimum Cost Minutiae Tree, Minutiae Pattern, Thermal Image, Minutiae Tree Traversal.

1.0 Introduction

In the past, a variety of methods had been used within the realm of individual identifying. Previously, the investigation relied on factors such as the individual's A/c quantity, Driving Licence and PAN (Permanently Accounts Information) card to establish their identity. However, these strategies proved to be ineffective and unsuccessful in accurately identifying an individual. Over time, many systems utilising human biographic identifiers were developed. Human biographical details, including their career, education, marital status, and address, were utilised as distinct identifiers for an individual. Currently, researchers are utilising biometric technologies for the purpose of individual authentication. Biometric methods rely on physiologic and behavioural characteristics. This approach utilised various biometric identifiers, including iris, hand vein, DNA matchmaking, face vein, palms a vein, cardiac pulse, fingerprints, voice recognition, and gait signatures [32].

Biometric features were scanned using specialised equipment such as Infrared Cameras (IR), Near Infra-Red (NIR), Low Wave Infrared (LWIR), Short-Wave Infra-Red (SWIR), and Mid-Wave Infra-Red (MWIR) cameras. Thermal pictures are employed to display the blood vessels and anatomical features of human facial veins. [6, 9, 10, and 14].

The thermal image displays temperature fluctuations in the blood vessels and tissues of a person's face. Physical contact is unnecessary for taking thermal photos of a person. Thermal pictures are also utilised for the detection of intricate disorders. Thus, thermal imaging are valuable in various domains such as engineering, medicine, space technology, and biomedical engineering. [2] [4]. Face

vein-based identification is a sophisticated method utilised for personal identification. The technique of facial vein-based identification involves capturing the thermal image of an individual using an infrared camera [3] [9]. Only infrared (IR) cameras have the capability to display the structures of facial veins and blood arteries that transport warm blood throughout the body, which is the primary reason why human skin feels warm. It has been noticed that each individual have a distinct facial vein structure, which aids in their identification. The process of obtaining images of face veins involves the employment of shallow and filtering procedures. The diameter of a facial vein typically ranges from 10 to 15 micrometres [33]. The facial veins are influenced by the influence of temperature and psychological stress due to their reliance on blood vessel circulation. The veins undergo structural and dimensional changes in response to an increase in body temperature. Tension is formed as a result of the expansion in veins. The diameter of veins is constricted as a result of tension, which significantly affects the circulatory system. Figure 1 [13] represents the sample of the real image, thermal image, face veins image, and thinned face veins patterns. This research introduces a novel method for identifying individuals based on the patterns of veins in their face. The suggested technique involves several crucial processes, including extracting facial veins from a thermal picture, thinning the face veins, generating a minutiae graph (MG) from the thinned face veins image, determining the lowest cost defilement tree (MCMT), navigating the MCMT, as well as corresponding the findings.

1(a) Actual image

1(b) Thermal image

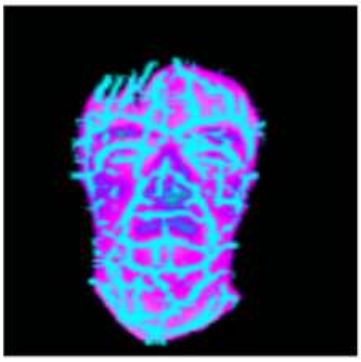

1(c) Face veins image

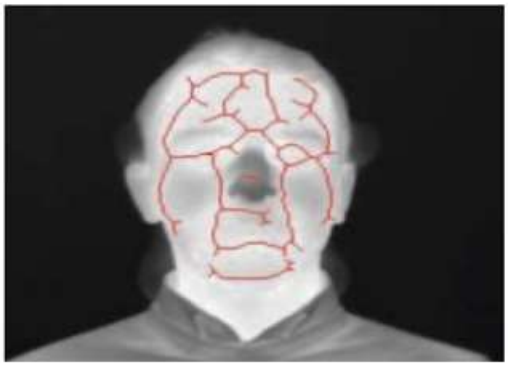

1(d) Thinned image

Figure 1 displays an illustration of a real picture, the thermal picture, a picture of facial veins, and a thinner version of the human face vein.

2.0 Literature Review

Mottl Vadim et al. employed the elastic translation technique to distinguish the distinct facial features of an individual using a two-pixel grid [22]. Shiguang Shan et al. introduced a method called the Face Specific Subspace technique, which is used to accurately detect the distinct facial features of individuals. The results were compared utilising the Yale Faces Collection. For the purpose of assessing the reliability, a total of 350 subjects were employed in this method [31]. Leonardo Trujillo et al. employed a method that involves extracting local and global features to address the challenges associated with face recognition. A Support Vector Machine (SVM) technique was utilised for face

classification [33]. Marc Garbey et al. employed a rapid Fourier transformation-based technique to identify the face and utilised the pulse rate to measure the temperature of blood vessels based on blood flow [9]. Gang Wang Jian et al. utilised infrared photos to extract facial traits of an individual. The researchers employed a face detection and feature extraction technique to analyse the facial veins of an individual [35].

Buddharaju Pradeep et al. employed thermal imaging to extract the facial veins and measure blood perfusion, similar to how finger veins are visualised using the vascular structure of the face [3]. Arandjelovic Ognegen et al. introduced a method that involved comparing visual images and thermal imaging using the principles of angle and data processing [2]. Chennamma and her colleagues introduced a Markov Random Field (MRF) model for the purpose of recognising human faces. The utilisation of the Markov Random Field (MRF) model entails creating a rough representation of an image and then comparing it to the actual photograph [6].

Martinez Brais et al. employed thermal pictures to discern the human face and utilised the Haar Wavelet Decomposition (HWD) approach to compare the eyes, nose, and mouth of different human faces [19]. Mekyska Jiri et al. introduced a thermal face segmentation technique for dividing thermal images into segments. The segmented thermal pictures were geolocated in order to identify individuals [20]. Gault Travis et al. utilised the LWIR camera to capture a thermal image. The study employed vessel selection, pulse measurement, and wavelet modification to conduct a multi-resolution analysis of thermal images [10].

Chen Cunjian and his colleagues employed thermal pictures and NIR images of human faces to determine gender using the LBHP approach. In this study, the researchers utilised Principal Component Analysis (PCA) and Gaussian Mixture Model (GMM) to identify the gender of human faces. The results demonstrated that this method effectively recognises the gender of individuals based on their facial features [5]. Cho Siu Yeung et al. created a model called TIFA, which utilises Fuzzy CMAC and Neural Network techniques to detect individuals based on their face veins [7]. The proposed method accurately discerns the identity of an individual. Hartung Daniel et al. employed hand veins and finger veins as a means of individual identification. He created and built the BVPR system, which utilises spectral minutiae patterns to address the issue of personal identification [14] [15].

Guzman Ana et al. devised a methodology in which a thermal image is recorded using the FLIRT approach. Identity verification was performed on the registered image using feature extraction, noise removal, image morphology, and thermal facial signature techniques [12]. Seal Ayan et al. employed a method based on Local Binary Patterns (LBP) and Haar Wavelet Transform (HWT) to achieve distinctive identification of individuals. This method involves converting the thermal image into a grayscale image, and then converting the grayscale image into a binary image. The binary image is compared with other images to verify its identity [27] [28] [26]. The thermal facial recognition system, created by [27] [28], consists of two components: image processing and classification. The researchers, Seal Ayan et al., conducted a detailed analysis of the minutiae points to compare the facial veins of two individuals [27] [28]. In this study, the researchers utilised a TFRS-based approach to calculate the minutiae points from the thermal image [30].

Sergey Chekmenev and his colleagues employed the superficial temporal artery technique to measure the vascular heart. They utilised multi-resolution wavelet-based signal analysis techniques to recover the arterial pulse wave [4]. Kuratate Takaaki et al. employed three-dimensional appearance images for the purpose of generating identification. The utilisation of the 3D appearance image extends to several applications such as robot navigation, object detection, and human-robot interaction. In this study, the mask-bot was employed to determine the gender of a humanoid robotics face [17]. Wong Wai and colleagues utilised the head curve geometry approach to extract images from thermal facial data [36]. Osia Nnamdi and his colleagues employed the MWIR technology to capture thermal images. The suggested method use fiducial points to compare several faces using the SIFT methodology [25].

Guzman et al. using a MWIR camera to get thermal pictures. The researchers employed a feature extraction method and utilised the FLIRT methodology to process the registered image. The approach suggested by Guzman et al. accurately identifies an individual [13]. Wang Ning and colleagues employed a Multi biometric system that utilises a complex fusion method to compare multiple faces with each other [34]. Amirthavalli and colleagues utilised a thermal vision camera to obtain a thermal image and employed an image morphology based thermal signature extraction technique for individual identification [1]. Negied Nermin et al. employed the thermal band technique based on the infrared spectrum to discern the identity of an individual. The temperatures of the facial veins' vasculature are crucial in distinguishing individuals [23].

Ghiassa Reza et al. utilised SWIR, MWIR, LWIR, and IR cameras to get a thermal image. These thermal pictures were utilised to capture the facial veins of individuals. Ghiassa Reza et al. employed the LBP, Wavelet Transform, and neural network processing and matching approaches to successfully recognise an individual [11].

Kumar Sanjith and his colleagues employed the MWIR technology to get thermal pictures. Prior to picture registration, a Gabor filter was employed. Additionally, a single reference image was selected for comparison with all other images [16]. Lavanya et al. employed thermal imaging to depict the vasculature and blood circulation. The vasculature generates heat as a result of blood circulation through the veins. The blood veins are utilised for the purpose of comparing the facial structures of two photographs, whether they belong to the same individuals or distinct individuals [18]. Nithyakalyani et al. introduced a human biometric system that uses facial features to uniquely identify individuals [24].

3.0 Theoretical framework for recommended methodology.

Suppose "U" be an all-inclusive set that contains a number of connections from five distinct sets for an individual. The representation consists of the elements {„A‟, „B‟, „C‟, „D‟, „E‟}, with each set containing the paired values of edges and vertices. The finer details of the facial veins graph are denoted by vertices („v‟), while the connections between these finer details are denoted by edges („e‟). The characters {„u‟, „e‟, and „v‟} are saved in all sets to denote the beginning vertex, edge length connecting vertices, and ending vertex of the face veins network.

$$A= \{(u_1, e_1, v_1), (u_2, e_2, v_2) \dots (u_n, e_n, v_n)\}$$

$$B= \{(u_1, e_1, v_1), (u_2, e_2, v_2) \dots (u_n, e_n, v_n)\}$$

$$C= \{(u_1, e_1, v_1), (u_2, e_2, v_2) \dots (u_n, e_n, v_n)\} \quad (1)$$

$$D= \{(u_1, e_1, v_1), (u_2, e_2, v_2) \dots (u_n, e_n, v_n)\}$$

$$E= \{(u_1, e_1, v_1), (u_2, e_2, v_2) \dots (u_n, e_n, v_n)\}$$

$$U= \{A \ U \ B \ U \ C \ U \ D \ U \ E\}$$

Industrial Engineering Journal
ISSN: 0970-2555
Volume : 53, Issue 4, No. 7, April : 2024

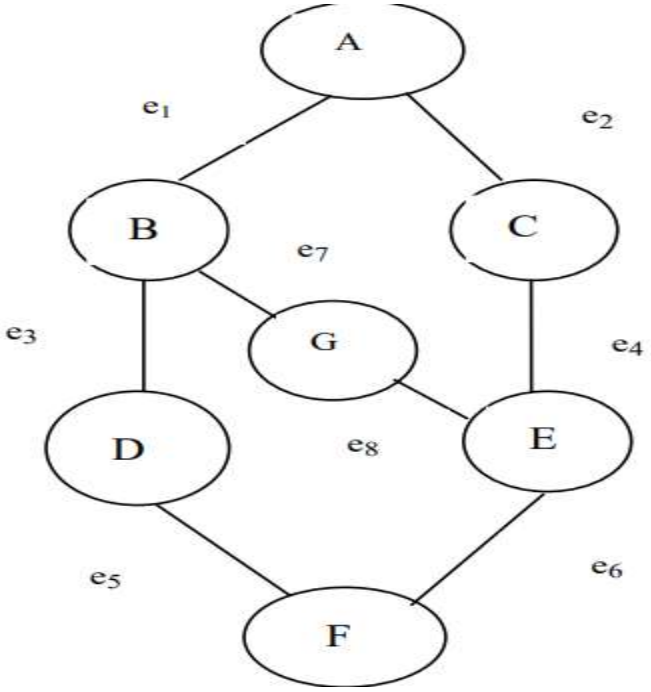

Figure 2 displays a visual depiction of the granularity graph of an individual.

2.1 Graphic Illustration of Minute details

The vertex edges of a facial veins picture are depicted as an equation known as the Small details Network (MG). A minutia graphs (MG) has multiple traversing trees, however just one of them is the Maximum Costs Minutia Trees (MCMT).

2.2 Description of the Minute details Trees

A minutiae graph's traversing tree is going to be referred to as the Granular Tree (MT). A minutia trees is going to be produced from MG, which will contain every one of MG's vertex but fails to create a single circuit.

Illustrations 2 and 3 depict the minutiae graph and matching granularity tree for an individual's facial arteries.

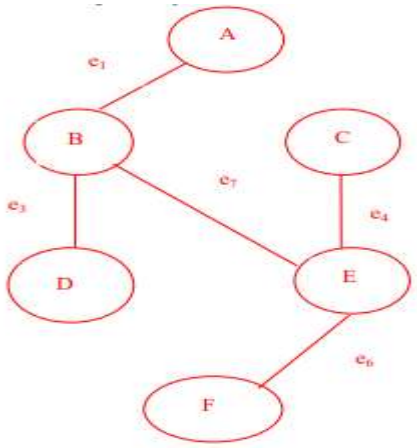

Figure 3: Schematic illustration of a minutia trees from the second diagram.

Theorem 1: Additionally, there is a specificity tree that corresponds to the layout of face capillaries for each individual. Evidence: The organisation of human face veins has resemblance to the vertices and edges depicted in figure 2. Each face vein is connected to specific spots, referred to as minutiae points or vertices.

The blood vessels that link small and precise places are referred to as edges. Let's examine a different graph shown in figure 4, where the vertices represent minutiae points and connecting veins of facial vein patterns, and the edges reflect the connections between them. Figure 4 displays

minutiae points labelled as vertices {„A‟, „B‟, „C‟, „D‟, „E‟, „F‟, „G‟}, and the connecting veins are represented as edges {„e1‟, „e2‟, „e3‟, „e4‟, „e5‟, „e6‟, „e7‟, „e8‟, „e9‟, „e10‟, „e11‟, „e12‟}. By referring to figure 4, we may conclude that blood circulates through veins, indicating the veins were interconnected. The interconnected veins are creating a tiny network. Every minutiae graph is guaranteed to have at least one spanning tree. Thus, the graph depicted in figure 4, known as the minutiae graph, possesses a minimum of one crossing plant.

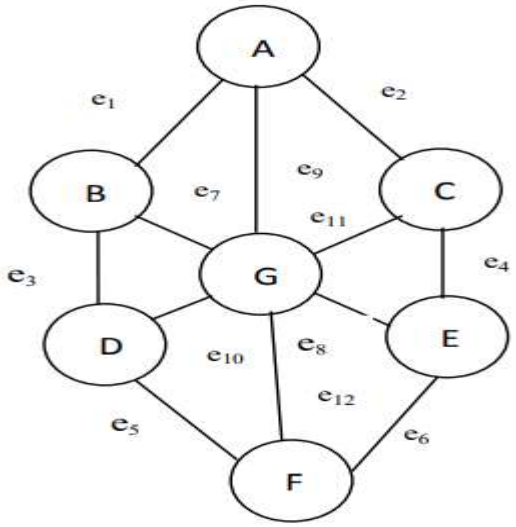

Figure 4: Schematic illustration of the minutia structure.

The facial veins of every individual are interconnected and form a minutiae graph (MG). Each MG possesses a spanning tree. The minimal spanning tree of a multigraph is referred to as the minutiae tree (MT). Consequently, it can be asserted that every individual's facial vein pattern will possess at least one unique marker.

Therefore, hypothesis 1 has been demonstrated.

Theorem 2 states that every MG has a unique Minimum Cost Minutiae Tree (MCMT). Evidence: Let "US" denote a universal set that encompasses the vertex and edge values of an MG (multi-graph). Consider a distinct collection {„W‟, „X‟, „Y‟, „Z‟} that represents various cost minutiae trees and contains the lowest edge values of the graph. The mathematical representation of the set "US" is given by equation (2).

$$US = \{(V_1, E_1), (V_2, E_2), \ldots (V_n, E_n)\} \qquad (2)$$

Various tree spans may be derived from Equation (2), or the routes taken by these spanning branches can be expressed using Equations (3), (4), (5), and (6).

$$W = \{P_2, P_4, P_6, \ldots \ldots P_{2n}\} \qquad (3)$$

$$X = \{P_1, P_3, P_5, \ldots \ldots P_{2n-1}\} \qquad (4)$$

$$Y = \{P_1, P_4, P_7, \ldots \ldots P_{3n-2}\} \qquad (5)$$

$$Z = \{P_2, P_6, P_{10}, \ldots \ldots P_{4n-2}\} \qquad (6)$$

In equations (3) through (6), P1, P2, ..Pn indicate various pathways of bridging trees, while 'W', 'X', 'Y', and 'Z' indicate distinct cost minimum cost maximum transmission units (MCMTs). Equations (7) to (10) are utilized to compute the boundary parameters of each least cost spanning trees (MCST).

Industrial Engineering Journal
ISSN: 0970-2555
Volume : 53, Issue 4, No. 7, April : 2024

$$S_1 = \sum_{i=1}^{n} W_i \quad (7)$$

$$S_2 = \sum_{i=1}^{n} X_i \quad (8)$$

$$S_3 = \sum_{i=1}^{n} Y_i \quad (9)$$

$$S_4 = \sum_{i=1}^{n} Z_i \quad (10)$$

In Kruskal's technique, the cheapest edges are chosen to form the minimal cost spanning trees. Hence, the pathways derived from equations (3), (4), (5), and (6) are going to be identical, and equations (7) to (10) will yield the same numerical values while traversing the roadway. Both the Prim or Kruskal's algorithms produce the same cheapest spreading tree (MCST), which is referred to as the minimum cost minimum spanning tree (MCMT) for a given graph. Hence, it may be asserted that there is a unique MCMT for every MG.
Therefore, the theory has been demonstrated.
The intricate configuration of MG for the facial venous patterns might be depicted by figure 5. Figure 5 depicts a graph where every vertex represents a minutia point of view, and individual minutia dots are linked together by edges. The distance between the two minutiae points is represented by the number of pixels along the edge. Equation (11) is utilized to compute the expense of the granularity structure.

$$Cost\ of\ MG\ (CMG) = \sum_{i=1}^{n} e_i \quad (11)$$

Let n be the entire amount all vertices in the MG MG, which is where n is greater than or equal to zero and less than n. Therefore, in any MG, the number of vertices will consistently be smaller than the number of edges.
Let's establish the variables that will be utilized to represent our suggested method for personal identification based on face veins. The following variables are: MT: Minutiae Tree, m: Number of edges in MT, n: Number of edges in MG, p: Number of vertices in MT, q: Number of vertices in MG, Vi represents the total number of vertices in the MT. Root vertices in machine translation (MT), Let Li represent the set of left vertices of a vertex in MT, Ri represent the set of right vertices of a vertex in MT, and ei represent the number of edges in MT. tmp: The overall count of minutiae points in a certain MT (Minutiae Template), mp: The specific count of minutiae points in the same MT. G: The total number of edges and vertices in a mathematical tree (MT) is: MCMTT refers to the process of traversing a minutiae tree with the lowest possible cost, whereas tsmcmt represents the total size of MCMT.

Industrial Engineering Journal
ISSN: 0970-2555
Volume : 53, Issue 4, No. 7, April : 2024

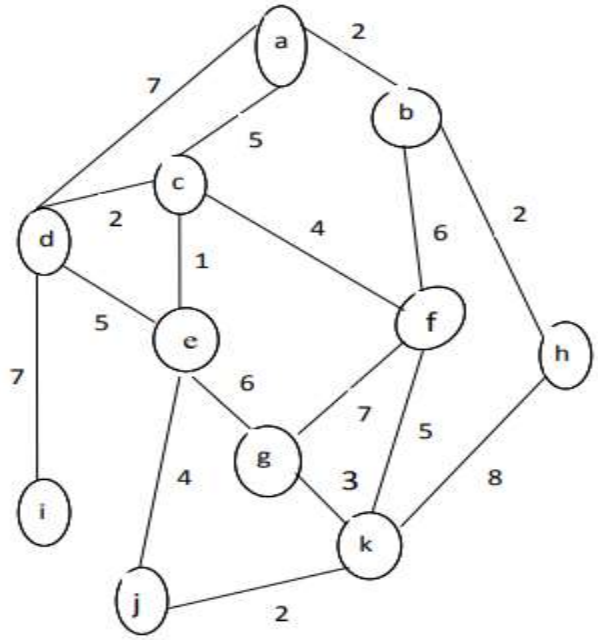

Figure 5 displays a visual depiction of the intricate arrangement of veins on an individual's body.
The detailed spots & their extremes for a facial vein network are depicted in Figure 5, wherein "a", "b", "c", "d", "e", "f", "g", "h", "i", "j", and "k" denote the specific spots. The numerical values in fig. 5 indicate the pixel distance between microscopic points in the depiction of face vein. To discover the Minimum Cost Maximum Tree (MCMT) for a Minimum Spanning Tree (MST) in a Multi-Graph (MG), we can utilize either Kruskal's or Prim's approach.
The minimum cost matching tree (MCMT) shown in figure 5 is depicted in figure 6. Figure 6 is derived by implementing Kruskal's technique on Figure 5. To retrieve the string used for authentication on the smart cards, the MCMT of figure 6 can be navigated in pre-ordering. Equation (12) denotes the aggregate quantity of minutiae elements within the specificity tree with the lowest cost.

$$tmp = \sum_{i=1}^{n}(RT_i,\ L_i, R_i) \qquad (12)$$

Equation (13) represents the price of a minutia branch.

$$CMT=\sum_{i=1}^{m} e_i \qquad (13)$$

In Equation (13), CMT represents the cost for a minutia tree, wherein 'm' is the maximum number of connections and 'n' is the number of vertices in an MT. It is important to note that 'm' is less than 'n'.
Equation (14) calculates the edge metrics for vertices once the crossing procedure is completed.

$$G= \sum_{i=1}^{p} \sum_{j=1}^{m} V_i[RT_j, L_j, R_j]e_i \qquad (14)$$

Researchers have previously demonstrated the type of MCMT depicted in figure 6 is distinct for each individual's facial vein arrangements.
Prim's approach, that is utilized to determine the minimal cost spreading tree, is able to be expressed as Equation (15).

$$M= \{(n, P[n]): n \in N-\{x\} -Q\} \qquad (15)$$

In Equation (15), the symbol "M" indicates an array which includes the smallest possible values of granularity. The symbol "P[n]" denotes one of the parent vertices on "{x}" denotes the root vertices

multiple and "{Q}" indicates the order of crossing all the edges and vertices of a Minimal Cost Matching Tree (MCMT).
If a Minimum Cost Maximum Flow (MCMT) graph has no edges or corners, then the value of the graph will be zero and the procedure will be completed. The finalization condition for our idea of an algorithm is given by Equation (16).

$$M = \{(n, P[n]): n \varepsilon N - \{x\}\} \quad (16)$$

Equation (17) represents the total expense of order ahead of time navigation for each of the borders and vertices in an MCMT.

$$tc = \sum_{i=1}^{n} e_i(n) \quad (17)$$

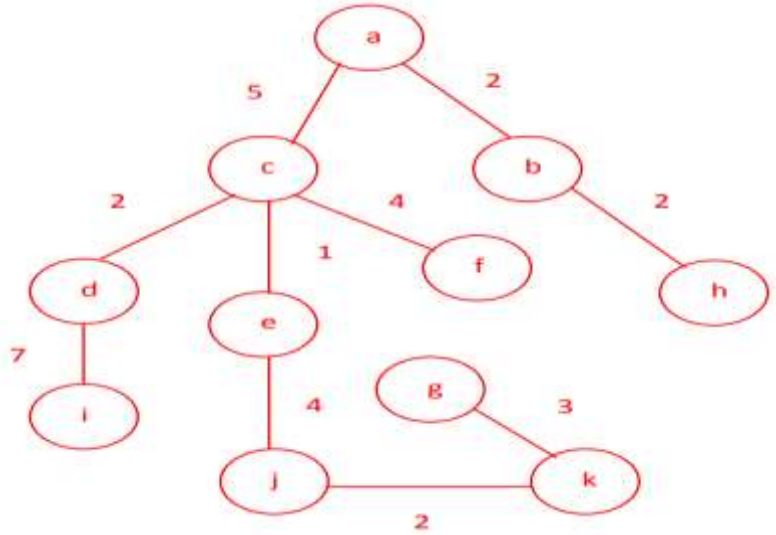

Figure 6 illustrates a visual depiction of the minimum price spanned branch.
Based upon these theoretical deductions and formulas, we may deduce that each individual possesses a distinct MCMT traverse. This sequence will be placed in an electronic depository for identifying an individual.

4.0 The proposed approach

Identification is presented in this part of the article. The suggested methodology employs a number of processes to process a thermal image from an individual's encounter:

Analyzing the thermal facial image of an individual

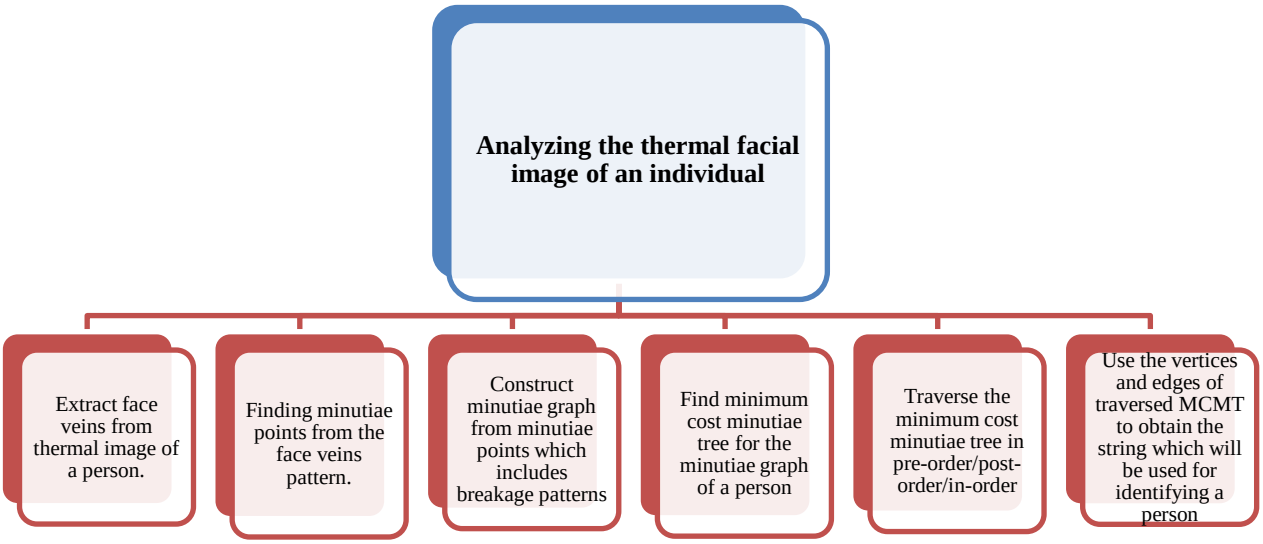

Industrial Engineering Journal
ISSN: 0970-2555
Volume : 53, Issue 4, No. 7, April : 2024

A. Infrared analysis of images for identifying facial vein

Once an image type was chosen, researchers continued collecting the characteristics of the thermal picture. The process of extracting face veins from a photograph of an individual involves a number of stages:

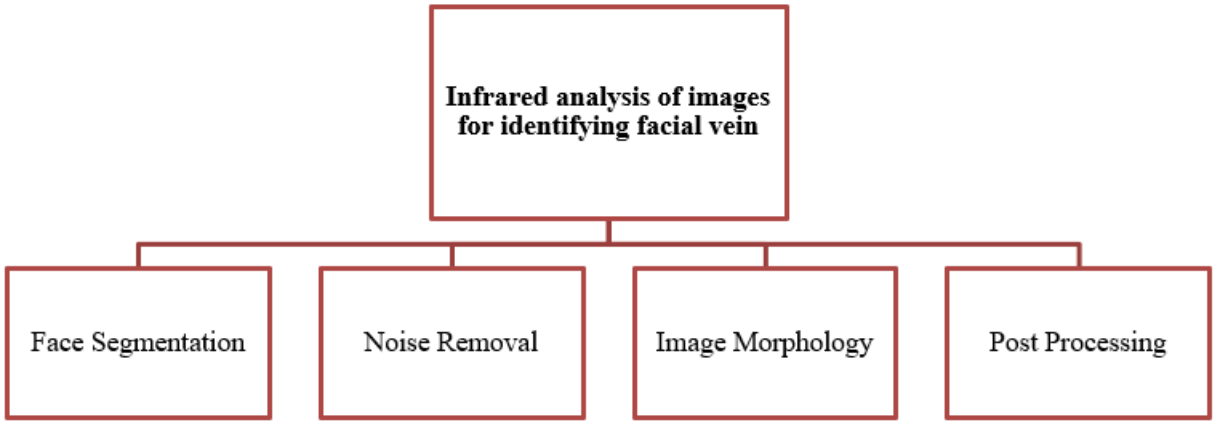

B. Detecting Specific details spots using the structure of an individual's facial vein.

A minutia network is an illustration where tiny locations are depicted as the vertices while the gap from two adjacent minutia locations is expressed by the width of the graph's edges. The method employed for extracting minutiae elements from the structure of facial veins utilizes thirty two scenarios. These scenarios are employed to obtain the vertex of a minutiae network, which will be depicted based on the arrangement of the veins on the skin of the face. Figure 7 displays the scenarios utilized for extracting minutia elements form the shapes of face veins. The specific details are achieved by utilizing instances using m1 to m24 in figure 7, whereas the locations where breaking occurs or the end vertex can be obtained using cases m25 to m32 in the identical image.

m1 = [0,0,1;1,1,0;0,0,1]; m2 = [0,1,0;0,1,0;1,0,1];
m3 = [1,0,0;0,1,1;1,0,0]; m4 = [1,0,1;0,1,0;0,1,0];
m5 = [1,0,0;0,1,1;0,1,0]; m6 = [0,0,1;1,1,0;0,1,0];
m7 = [0,1,0;1,1,0;0,0,1]; m8 = [0,1,0;0,1,1;1,0,0];
m9 = [0,0,0;1,1,1;0,1,0]; m10 = [0,1,0;1,1,0;0,1,0];
m11 = [0,1,0;1,1,1;0,0,0]; m12 = [0,1,0;0,1,1;0,1,0]
m13 = [1,0,1;0,1,0;1,0,0]; m14 = [1,0,1;0,1,0;0,0,1];
m15 = [0,0,1;0,1,0;1,0,1]; m16 = [1,0,0;0,1,0;1,0,1];
m17 = [0,1,0;1,1,1;1,0,0]; m18 = [0,1,0;1,1,1;0,0,1];
m19 = [1,0,0;1,1,1;0,1,0]; m20 = [0,0,1;1,1,1;0,1,0];
m21 = [0,1,0;0,1,1;1,1,0]; m22 = [1,1,0;0,1,1;0,1,0];
m23 = [0,1,1;1,1,0;0,1,0]; m24 = [0,1,0;1,1,0;0,1,1];
m25 = [1,0,0;0,1,0;0,0,0]; m26 = [0,1,0;0,1,0;0,0,0];
m27 = [0,0,1;0,1,0;0,0,0]; m28 = [0,0,0;0,1,1;0,0,0];
m29 = [0,0,0;0,1,0;0,0,1]; m30 = [0,0,0;0,1,0;0,1,0];
m31 = [0,0,0;0,1,0;1,0,0]; m32 = [0,0,0;1,1,0;0,0,0];

Figure 7. The instances from which detail elements were extracted from facial veins

C. Minimal Costs Details Trees (MCMT) Determination from the Details Diagram

The neighboring minutia elements acquired by implementing the criteria outlined in figure 7 are connected to form the small details network. Next, the details of the network will be provided as input to create the Maximum Cost Minutia Trees (MCMT). The procedure for creating an MCMT (Minutiae-Centered Matching Template) from a granularity line chart is illustrated in figure 8.

Industrial Engineering Journal
ISSN: 0970-2555
Volume : 53, Issue 4, No. 7, April : 2024

```
Input:  Minutiae Graph
Output:  Minimum Cost Minutiae Tree
1. Algorithm Minimum_Cost_MT(minutiae graph )
        {// assume that g has at least one vertex
2. mpv={0};  // start with vertex 0 and no edge
3. for (t=0; t contain fewer than e-1edge; add (ui, vi) to t)
        {
4. Let (ui,vi) be a minimum cost edge such  that ui is the
element of mpv and vi is not the element of mpv;
5.  If (there is no edge) break;
6.  { Add vi to mpv;}
        } // End of for loop
7.  if (t contains fewer than e-1 edge)
8. { printf (" minutiae point";}
        } // End of algorithm
```

Figure 8: Methodology for determining the smallest Cost Minute details Trees.

In figure 8, the sign "g'" indicates at least a single vertex in the minutia network. The symbol "t" represents the number of vertices in the minutiae structure. The symbol "ui" indicates the initial vertex, while "vi" denotes.

The symbol "v" indicates the terminal vertex, and "ei" symbolizes a boundary between polygons.

D. Generating Identity Strings using MCMT.

To obtain the identifying string, we can traverse the MCMT in reservation, subsequent, and in-order. However, in the studies we conducted, we employed a pre-order traversing-based strategy to create an identifiable string since it is faster compared to other traversing methods.

The identifying vector will contain MCMT polygons and line lengths of time. Figure 9 shows the procedure used to detect the vertex and edge regions of a visited string using MCMT.

```
Input: Minimum Cost Minutiae Tree.
Output: Traversal string of vertices and edges.
1. Algorithm Minutiae_Tree_Traversing_Procedure
(minutiae tree)
        { // Traversal process of Minutiae Tree
2. preorder(r);
3.  preorder(MTNode *CurrentNode)
                    // the traversal preorder traverse the
        { if (CurrentNode)
4.   { printf (CurrentNode→data);
5.    preorder (CurrentNode→leftChild);
6.    preorder (CurrentNode→rightChild);
        }} }
```

Figure 9: The crossing of the Minimal cost minutia trees.

In figure 9, the symbol 'r' denotes the base facet of the minutia trees. The term 'CurrentNode' refers to the specified minutiae points on the MCMT, while 'leftChild' symbolizes the vertices on the left hand side of its MCMT, and 'rightChild' symbolizes the vertices on the right flank of the MCMT. Each individual will possess a distinct MCMT reservations traverse value referred to as a "association string." The string will be utilized in the internal storage of the chip in the smart card all additional verification purposes.

E. Findings & Examination of Experimentation Data

In order to evaluate the efficacy of the suggested methodology, it is necessary to carry out these procedures:

Industrial Engineering Journal
ISSN: 0970-2555
Volume : 53, Issue 4, No. 7, April : 2024

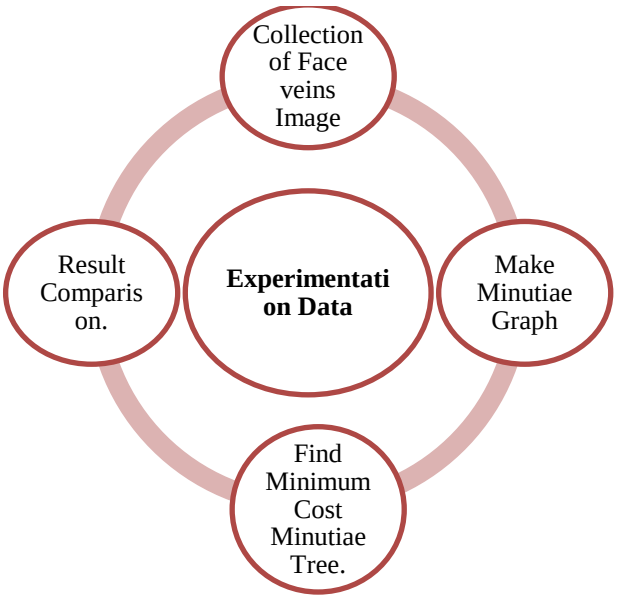

The procedures are outlined in paragraph A, B, C, and D within the fifth part of this document. In addition, subsections F, E, and G provide an in-depth examination of the outcomes and examine the contrasting characteristics of the suggested method to other established procedures.

(i) Actual image

(ii) 90^0 right rotation

(iii) 180^0right rotation

(iv) 270^0 right rotation

Industrial Engineering Journal
ISSN: 0970-2555
Volume : 53, Issue 4, No. 7, April : 2024

(v) 90^0 left rotation

(vi) 180^0 left rotation

(vii) 270^0 left rotation

(viii) 315^0 left rotation

Figure 10(a) Picture of the veins in the exterior of the first subject rotated at various angles

(I)Actual image

(ii) 90^o right rotation

(iii) 180^o right rotation

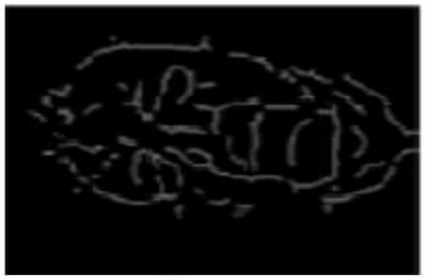

(iv) 270^o right rotation

(v) 90^0 left rotation

(vi) 180^0 left rotation

(vii) 270^0 left rotation

(viii) 315^0 left rotation

Figure:10(b) A picture of the vessels on the face of another individual rotated at any angle

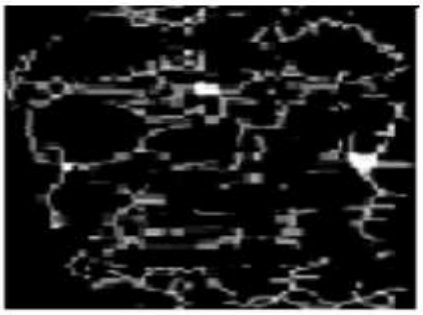

(i) Actual Image

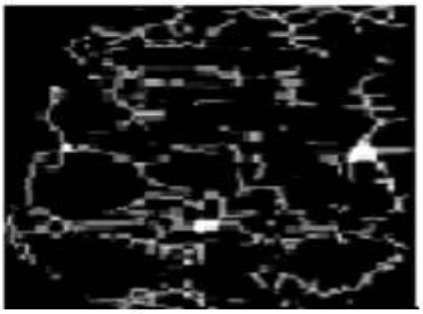

(ii) 90^0 right rotation

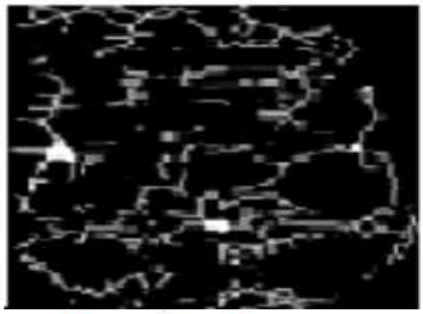

(iii) 180^0 right rotation

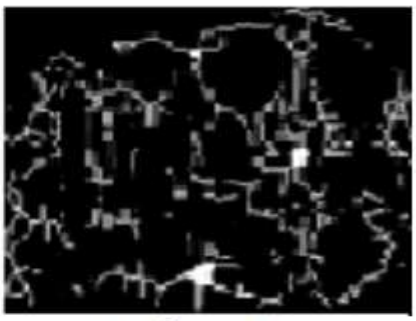

(iv) 270^0 right rotation

Industrial Engineering Journal
ISSN: 0970-2555
Volume : 53, Issue 4, No. 7, April : 2024

(v) 90^0 left rotation

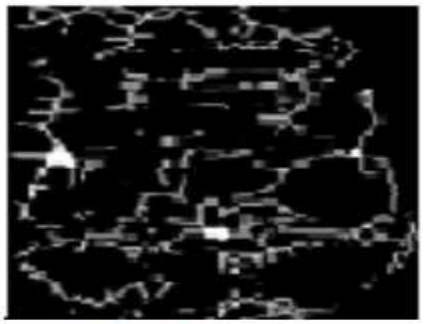

(vi) 180^0 left rotation

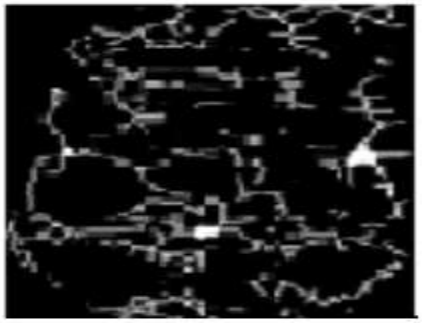

(vii) 270^0 Left rotation

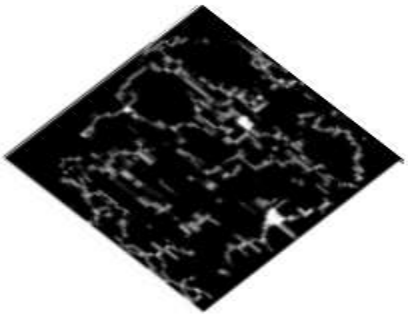

(viii) 315^0 left rotation

Figure:10(c) Responsive venous image of an additional individual at various angles of rotation

(i) Actual Image

(ii) 90^0 right rotation

(iii) 180^0 right rotation

(iv) 270^0 right rotation

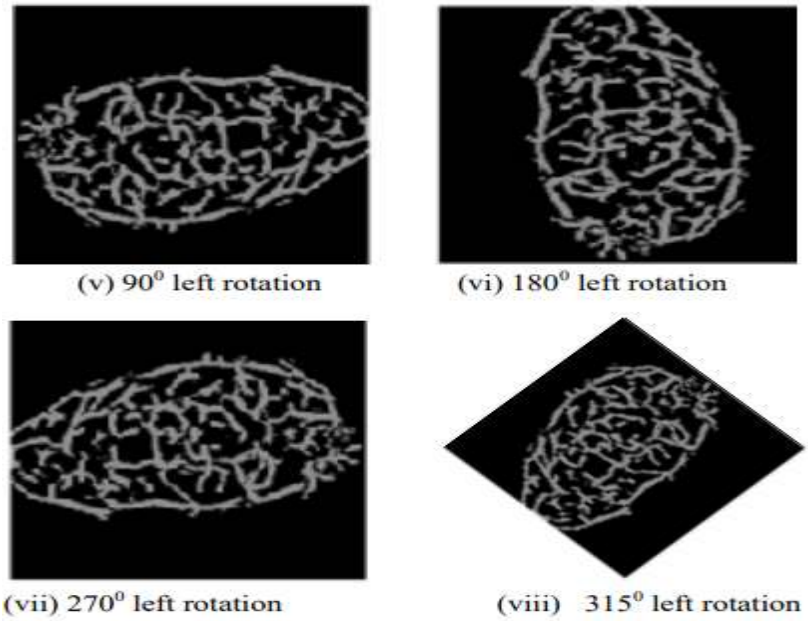

Figure: 10 (d) a picture of the vessels on the face of the 4th individual at various angle of rotation.

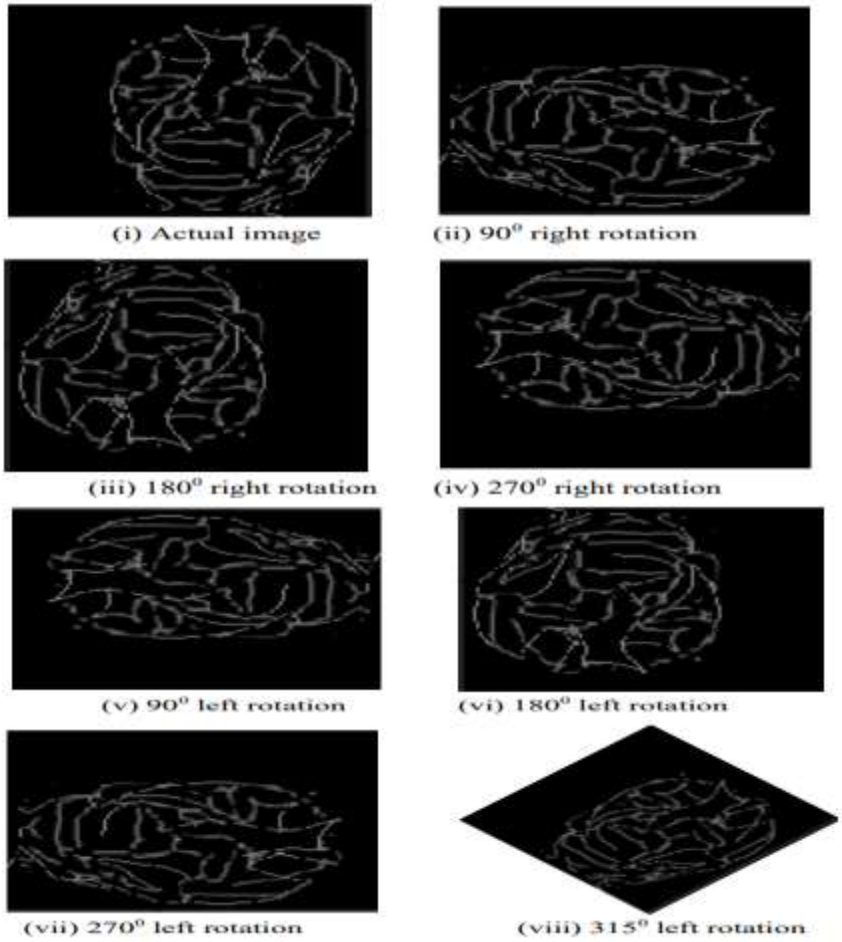

Figure: 10 (e) Illustration of the fifth the individual's facial veins rotated at various angles.

A. Assortment of Facial Veins Images

During this stage, the Infra-Red (IR) sensor is employed to capture temperature pictures. The Perona-Malik-Anisotropic filter is used to detect the picture of facial veins [13]. For testing purposes, we have captured eight photographs of the same person's facial veins at various degree rotation. Our data set contains a total of five individuals' pictures.

Industrial Engineering Journal
ISSN: 0970-2555
Volume : 53, Issue 4, No. 7, April : 2024

The size of each picture must be 120 pixels by 120 pixels. The pictures are shown in figures 10(a), 10(b), 10(c), 10(d), and 10(e).

B. Developing Minute details Networks using Facial Vein Images

Once the picture of the facial veins is located, a MATLAB application is used to create a graph of the minutiae. During our investigation, researchers conducted operations on a picture that had to have dimensions of 120 by 120 pixels. The process of generating a minutia network using the structure of an individual's facial veins involves the following procedures:

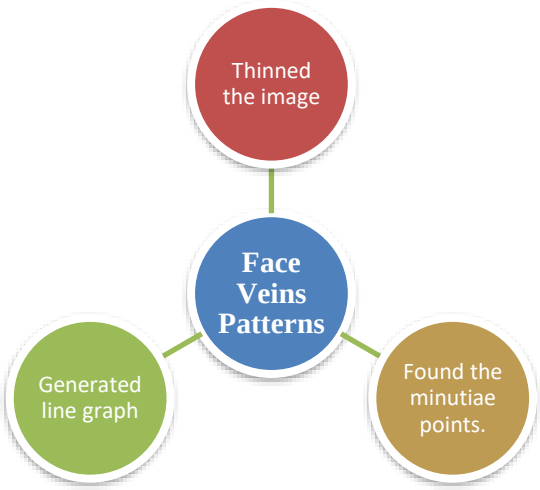

The picture of the facial veins is transformed into a binary image, which consists of just black and white pixels, using the MATLAB procedure im2bw(image, level). Then, the algorithm bwmorph(image, 'choice', grade) is executed to produce the thinning photographs seen in figure 11.

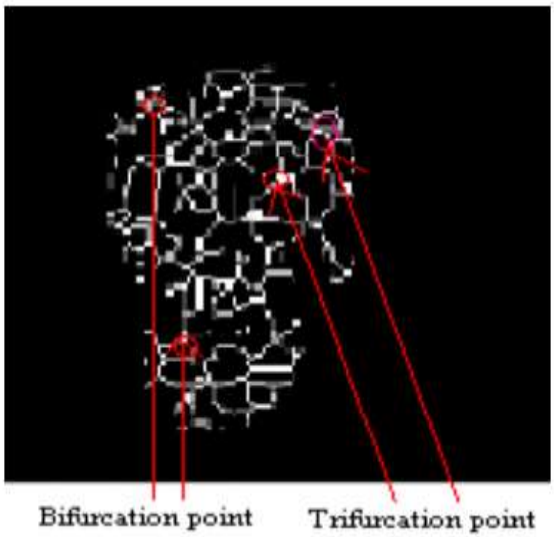

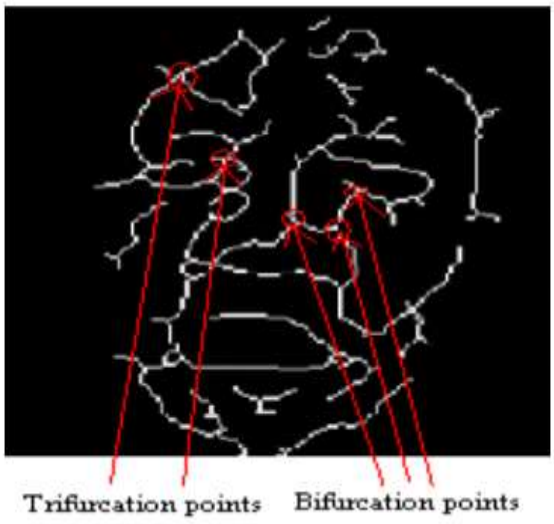

Industrial Engineering Journal
ISSN: 0970-2555
Volume : 53, Issue 4, No. 7, April : 2024

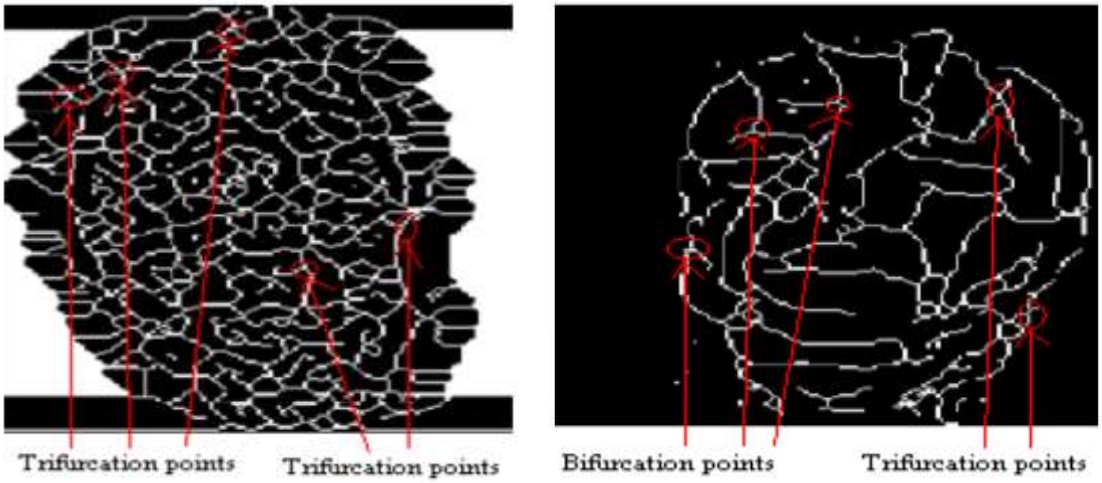

Figure 11 shows a reduced picture of several people based on their facial venous characteristics.
The reduced pictures in fig. 11 demonstrate the presence of bifurcation/trifurcation sites & breaking points in every reduced picture. The spots where facial veins patterns split into two or three branches will be regarded as the minutiae points. The MCMT may be derived from a minutiae graph representing the patterns of facial veins.
If neither Kruskal's or Prim's approach is used to discover the minimum cost maximum tree (MCMT) using a minutia graph, the identical MCMT will be found for all rotations of the minutiae graph. Consequently, capturing photos of an individual's facial veins from various angles should yield identical MCMT (Mean Curvature Mapping Technique) values for figure 11. Therefore, we have selected the first picture of the facial veins for each individual from figure 11 to be used in additional research.
We used the clean(), close(), majority(), branchpoints(), and shrink() operations on the thinned picture of figure 11 in order to get the minutiae points of figure 12. Upon careful examination of the intricate details in figure 12, it is evident that each facial vein pattern has an estimated range of 80 to 200 minutiae points. The details in fig. 12 indicate that the pattern of veins on each person's face has a distinct and unique collection of details.

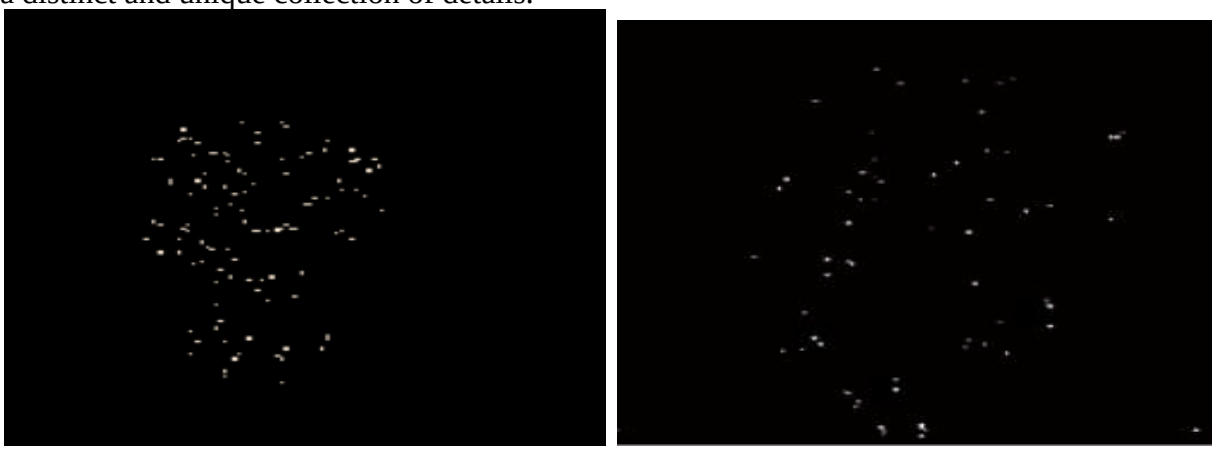

Industrial Engineering Journal
ISSN: 0970-2555
Volume : 53, Issue 4, No. 7, April : 2024

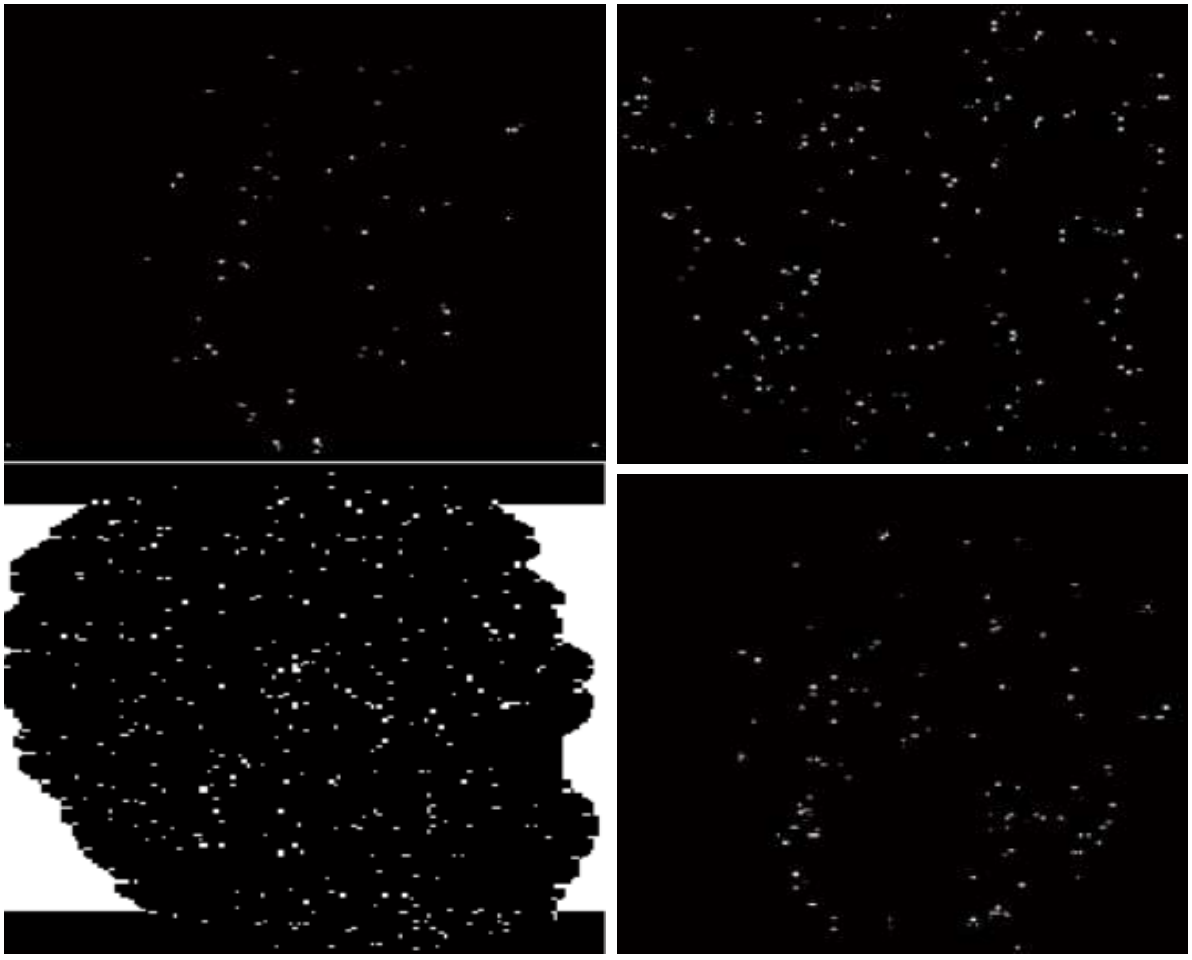

Figure 12: The vertices for granularity diagram representing various individuals

Producing Line Charts Using the Point of Minute details

Once detail elements have been generated for a picture of constricted facial vessels, they can be connected to form a line chart. The scant (image) function of the MATLAB program is employed to determine the measurements of individual minutia points, while the function for plotting (X coordinate, Y coordinate) is utilized to produce the line graph. Figure 13 illustrates the line graph that was produced to represent the smallest points for every person, as shown in Figure 12.

Fig. 13's graphs of lines indicate that the facial capillaries of each individual have a distinct line graphing.

The graphical graphs depicting the blood vessels on each individual's visage are entirely unique.

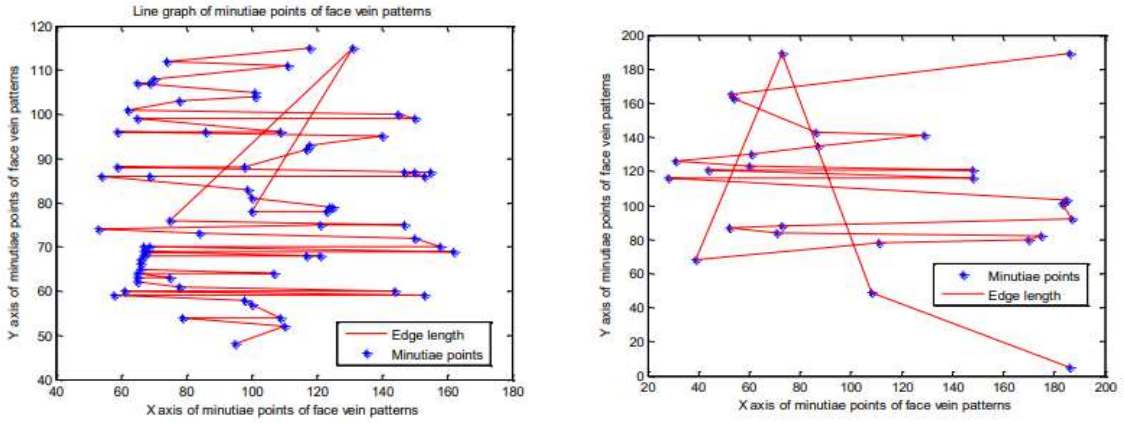

Industrial Engineering Journal
ISSN: 0970-2555
Volume : 53, Issue 4, No. 7, April : 2024

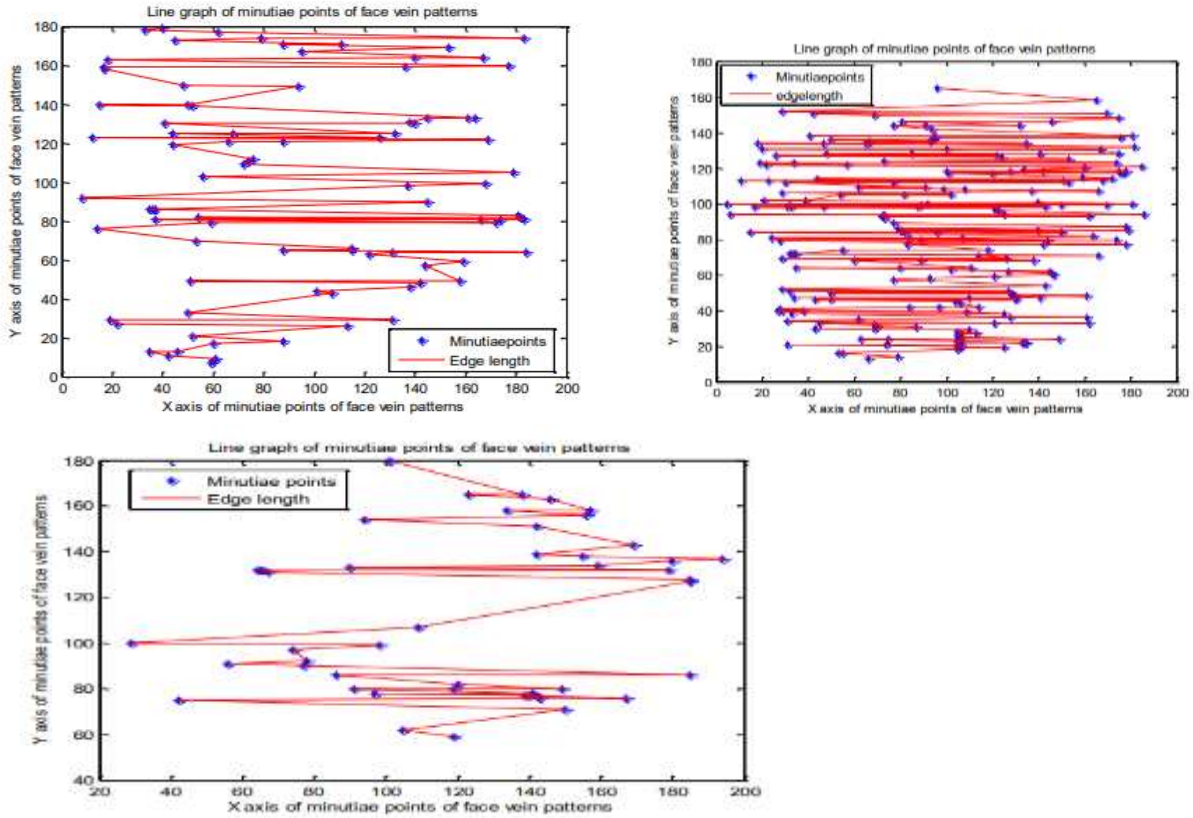

Figure 13: a line chart of various individuals

The following illustration demonstrates that every person has a distinct line graph, formed by linking the closest small details.

The detailed graphs of the image 12 and the linear graph in the thirteenth figure are valuable for developing the MCMT.

Developing the MCMT utilizing the Minute details network

The closest minutia elements are linked together using the line() algorithm in MATLAB to create a minutia trees having the lowest possible cost. The granularity points of fig. 12 are shown in fig. 14 by the use of MCMTs. Upon evaluating the findings of figure 14, it becomes evident that each individual has a distinct MCMT (Mean Cross Match Time). Furthermore, while examining the facial veins of the same individual, various MCMT values are obtained. The Multiway Compressed Merkle Trees (MCMTs) shown in figure 14 may be explored in pre-order, subsequent, or mid-order to produce the last a string, that is able to be utilized to serve additional identifying purposes.

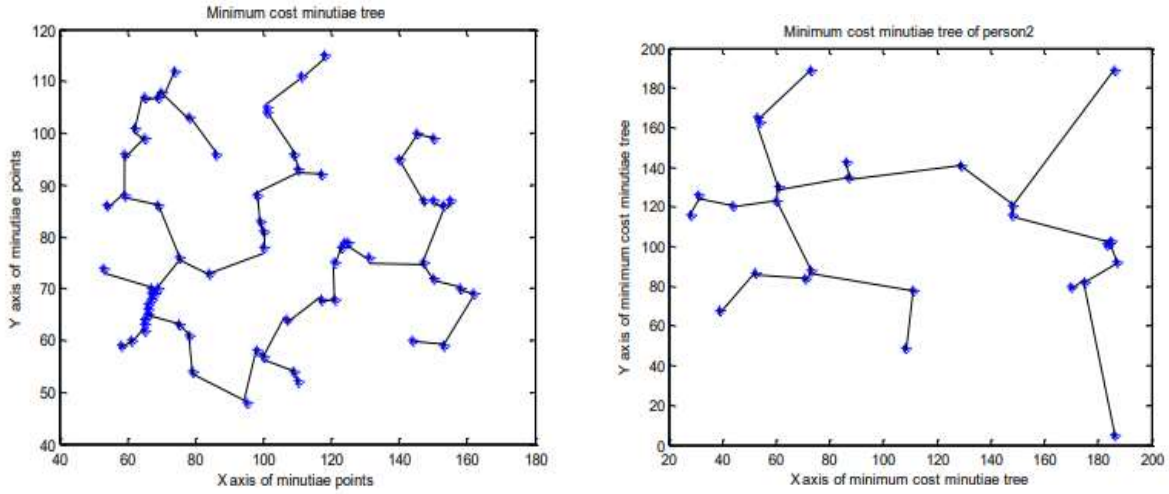

Industrial Engineering Journal
ISSN: 0970-2555
Volume : 53, Issue 4, No. 7, April : 2024

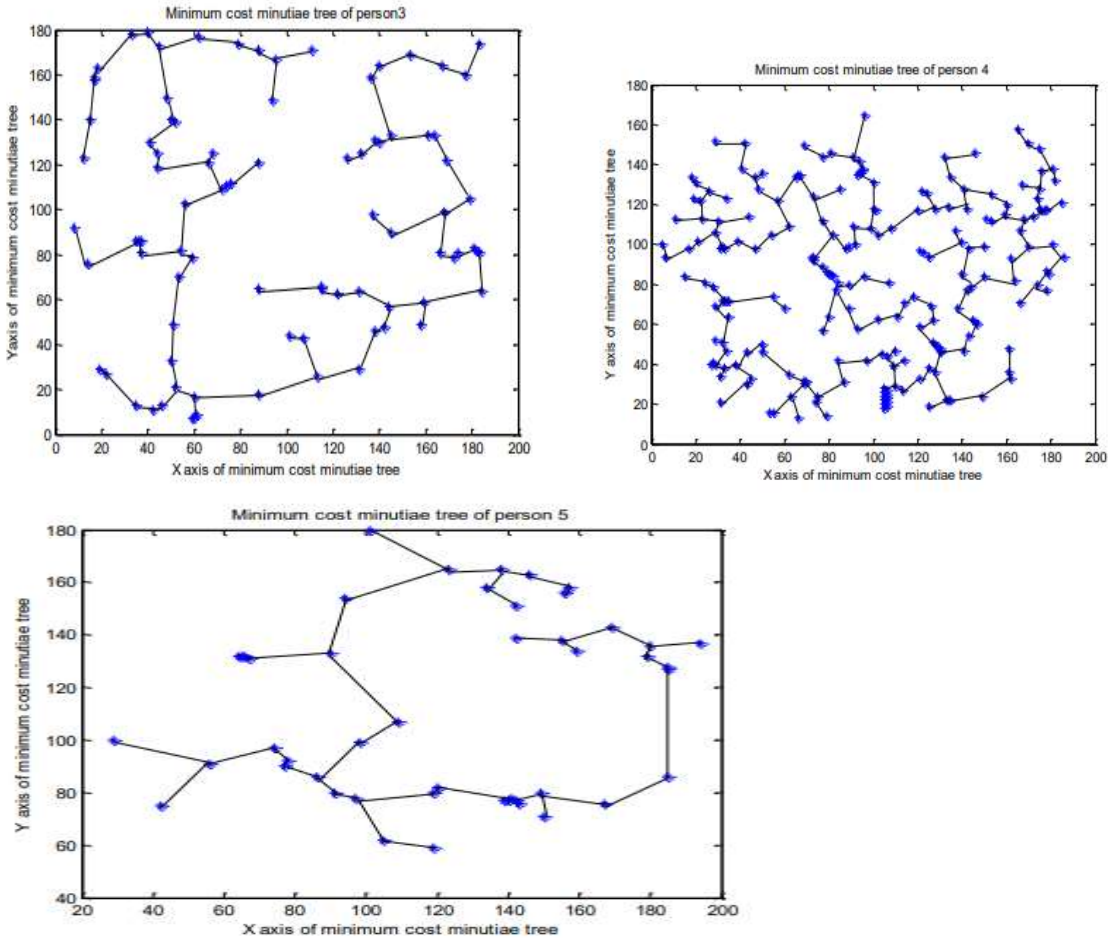

Figure 14: Minimal Price Details Trees with Various Individuals.

Traversing MCMT and contrasting outcomes

We employed pre-order traversing to traverse the MCMT shown in Fig. 15. A vertex is chosen as the first vertex. Figure 15 illustrates the direction and sequence of vertices visited, as well as the outcomes of the traversal.

The topmost vertex form the uppermost port of the trees is chosen as the starting point. Figure 15 shows the initial vertex as a rectangle. When traversing an MCMT in pre-order, we use vertices and edge lengths to create the substring.

A pre-order traversing for MCMT in figure. 15 involve several steps:

- **Step-I** • Traverse the root vertex in pre-order
- **Step-II** • Traverse the left edge and the left node inpre-order
- **Step-III** • Traverse the right edge and right node of MCMT in pre-order.
- **Step-IV** • Repeat the steps from step I to step III until all the vertices and edges are not traversed.

Industrial Engineering Journal
ISSN: 0970-2555
Volume : 53, Issue 4, No. 7, April : 2024

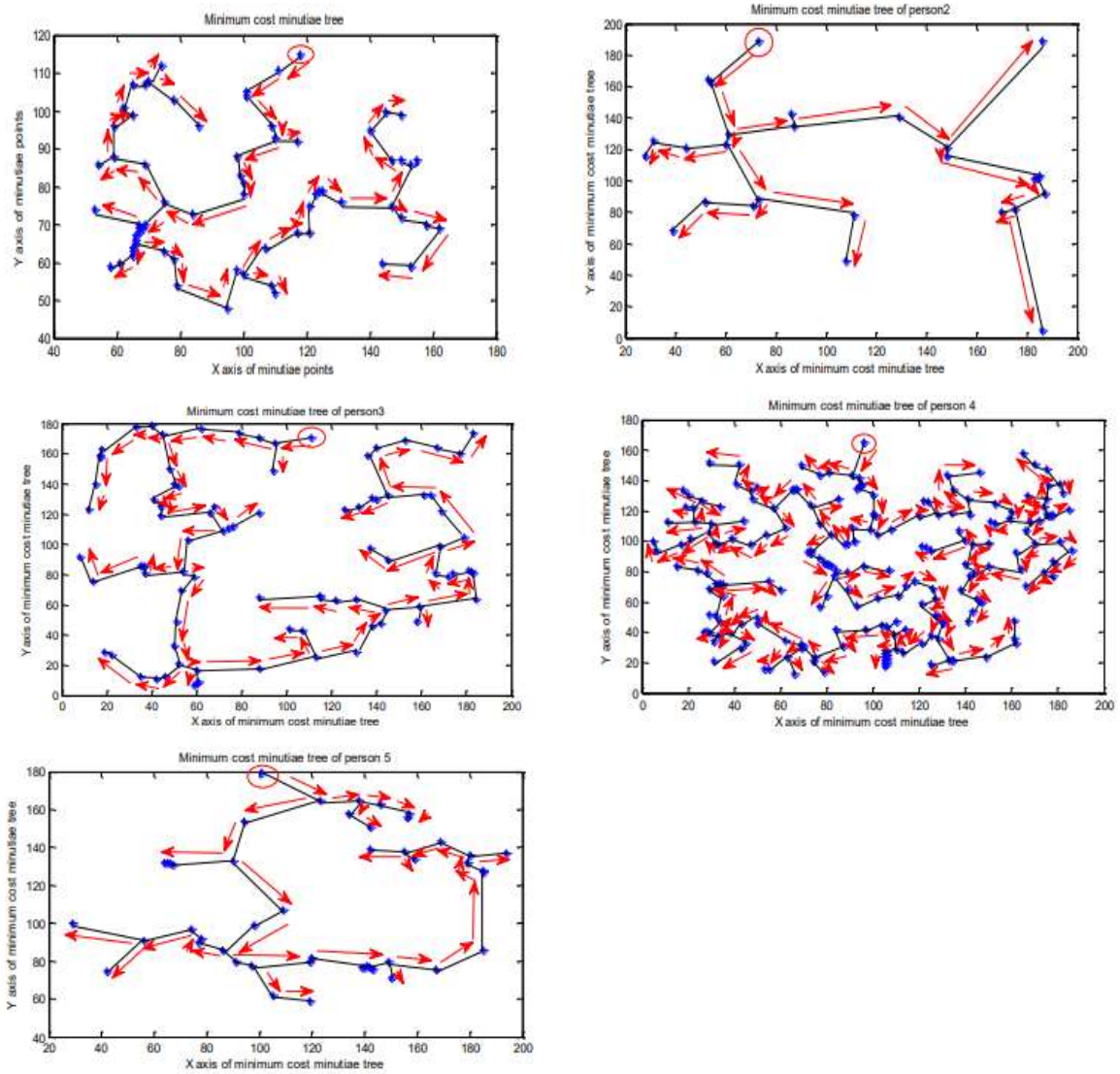

Fig. 15: Pre-ordering traverse string towards minimizing costs in minutia tree of distinct individuals.

The reservations traverse and the related visualization in figure 15 demonstrate that the framework of every individual's facial veins is distinct from the reservations traverse of MCMTs.

Developing code into the form of strings using MCMT

Upon concluding this traversal procedure, i developed an array of coding for MCMT, which allows for comparison of the facial vein patterns between two individuals. Through experimentation, it has been shown that every individual possesses a distinct set of string code values. Prior to creating the string of code numbers, it is necessary to determine the length of the edges that connect the edges.

The coordinates of the vertices and the matching values of the border lengths for the Minimum Convex Multidimensional Trees (MCMTs) shown in figure 15 are provided in figure 16. The red highlighted vertices in figure 16 indicate the initial vertex. The initial vertices will be utilized for pre-order traversal and will be crucial in creating the MCMT traverse strings.

Industrial Engineering Journal
ISSN: 0970-2555
Volume : 53, Issue 4, No. 7, April : 2024

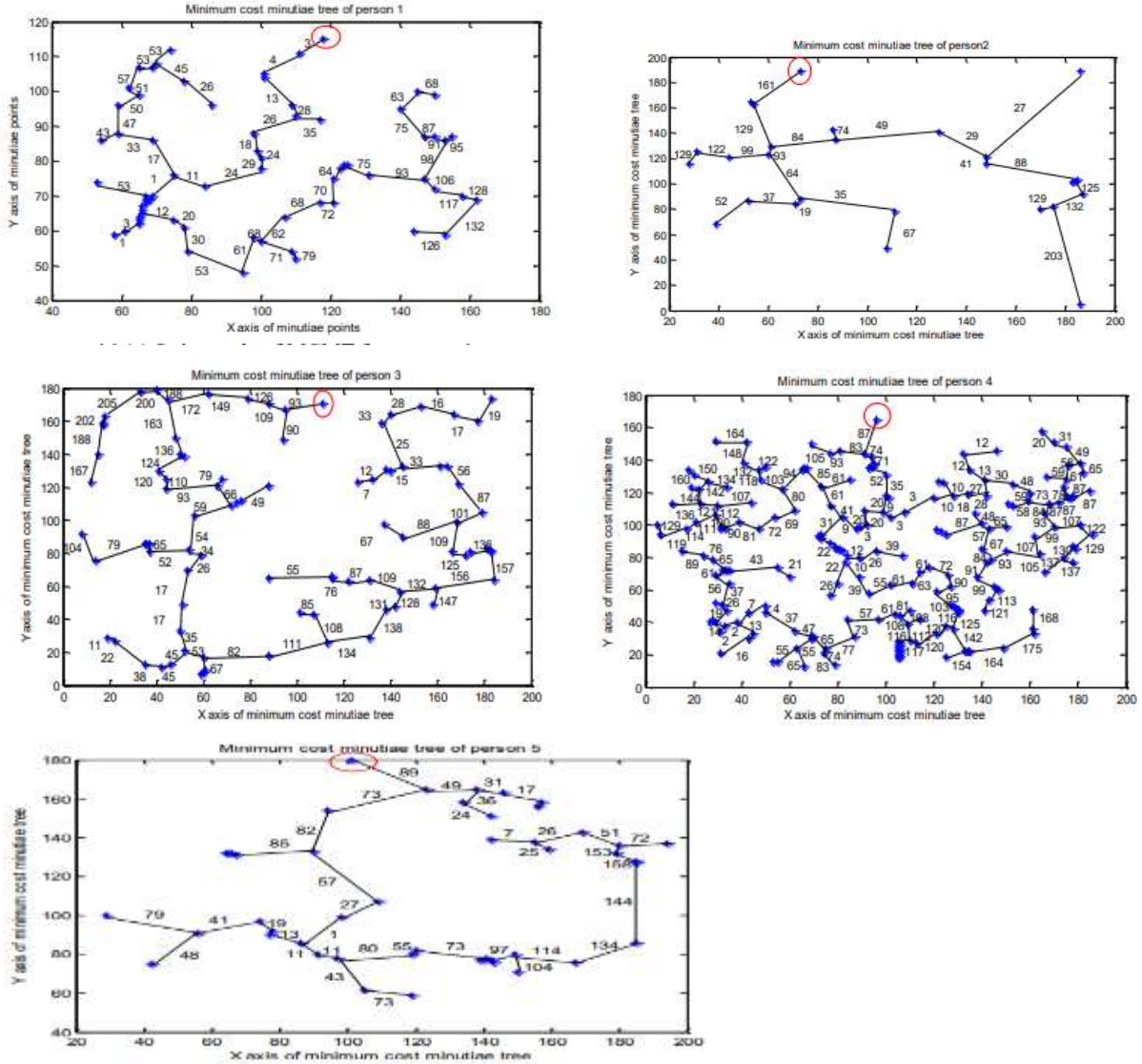

Figure 16 displays the lines of coding of a few minutiae tree for various individuals.

In picture 16, the total amount of lines in an MCMT will be one less than the amount of the vertices denoted as 'n'. The variable "n" is crucial in compressing the structure of an individual's facial capillaries.

Comparing of Various Individuals Utilizing Strings Coding

During this step, we check the purchased visited vertex & edge width data (represented as strings) of one individual to that of another individual. We varied the length of the edge parameters within the range of -5 to +5 in a synthetic scenario to conduct durability tests. In addition, we noticed that when the difference in edge length values for a person is less than -5 or greater than +5, the matching outcomes fall significantly. If the string of corresponding to two individuals have an identical percent in excess of 80% for the facial veins structure, it indicates that each of the strings are associated with a single individual. If the match rate is under 80%, we conclude that the facial vein patterns belong to distinct individuals in other instances.

Our investigations revealed that the comparable proportion of facial veins MCMT traversing string for two separate people is less than 30%, but for the same individual it exceeds 80%. The figure 17 displays the vertices and edge lengths for pre-order traversal of MCMTs.

Industrial Engineering Journal
ISSN: 0970-2555
Volume : 53, Issue 4, No. 7, April : 2024

P1={(1,3), (2,4), (3,13), (4,28), (5,26), (6,18), (7,24), (8,29), (9,24), (10,11), (11,17), (12,33), (13,47), (14,50), (15,51), (16,57), (17,53), (18,45), (19,26), (20,53), (21,43), (22,53),(23,3), (24,1), (25,12), (26,20), (27,30), (28,53), (29,61), (30,68), (31,71), (32,79), (33,62), (34,68), (35,72), (36,70), (37,64), (38,75), (39,93), (40,106), (41,117), (42,128), (43,132), (44,126), (45,98), (46,95), (47,91), (48,87), (49,75), (50,63), (51,68), (52,35)}

17(a) The vertices & line lengths of MCMT traverse per individual

P2={(1,161,), (2,129), (3,93), (4,99), (5,122), (6,129), (7,64), (8,19), (9,37), (10,52), (11,35), (12,67), (13,84), (14,49), (15,29), (16,41), (17,88), (18,125), (19,32), (20,129), (21,203), (22,27), (23,74)}

17(b) The triangles & line lengths of MCMT traverse per individuals

P4={(1,87), (2,83), (3,93), (4,105), (5,74), (6,71), (7,52), (8,35), (9,20), (10,20), (11,20), (12,3), (13,9), (14,41), (15,61), (16,61), (17,85), (18,94), (19,103), (20,118), (21,122), (22,132), (23,148), (24,164), (25,80), (26,69), (27,72), (28,81), (29,90), (30,100), (31,112), (32,107), (33,121), (34,136), (35,111), (36,114), (37,119), (38,129), (39,31), (40,22), (41,22), (42,26), (43,10), (44,39), (45,55), (46,61), (47,63), (48,61), (49,72), (50,90), (51,95), (52,103), (53,116), (54,120), (55,120), (56,112), (57,116), (58,117), (59,108), (60,61), (61,57), (62,73), (63,77), (64,74), (65,65), (66,55), (67,55), (68,65), (69,47), (70,37), (71,4), (72,7), (73,7), (74,2), (75,14), (76,19), (77,26), (78,37), (79,56), (80,61), (81,65), (82,76), (83,89), (84,43), (85,21), (86,2), (87,13), (88,16), (89,65), (90,83), (91,142), (92,154), (93,164), (94,175), (95,178), (96,168), (97,12), (98,26), (99,39), (100,9), (101,3), (102,3), (103,10), (104,10), (105,18), (106,28), (107,27), (108,13), (109,12), (110,12), (111,30), (112,48), (113,59), (114,58), (115,73), (116,84), (117,93), (118,99), (119,107), (120,105), (121,93), (122,84), (123,67), (124,57), (125,48), (126,87), (127,65), (128,91), (129,99), (130,99), (131,113), (132,121), (133,107), (134,122), (135,129), (136,130), (137,137), (138,137), (139,87), (140,87), (141,78), (142,59), (143,61), (144,58), (145,49), (146,31), (147,31), (148,20), (149,65), (150,87)}

17(d) The vertices & edges lengths of MCMT traverse over individual_4.

P5={(1,89), (2,73), (3,82), (4,85), (5,57), (6,27), (7,1), (8,13), (9,19), (10,41), (11,79), (12,48), (13,11), (14,11), (15,43), (16,73), (17,80), (18,55), (19,73), (20,97), (21,104), (22,114), (23,134), (24,144), (25,158), (26,153), (27,51), (28,26), (29,7), (30,25), (31,72), (32,49), (33,36), (34,24), (35,31), (36,17)}

17(e) The vertices & edges width parameters for MCMT traverse for individual_5.

Fig.17. Triangles and edges height environments for MCMT traverse vary by individual.

Figure 17 depicts vertices and edge lengths using integer values. In Fig. 17, the first integer number indicates vertices, while the second represents edge length. If each integer value of MCMT takes up two bytes of memory, the entire quantity of memory would be equivalent to traversing a person's facial veins.

VI CONCLUSIONS

The current effort introduces a novel approach for recognizing persons via facial the veins, using the MCMT traversal. Experiments have shown that every individual possesses a distinct Multichannel Multi-Timescale (MCMT) resulting in a unique string code representing their facial vein pattern. An individual's identification may be determined by analyzing the MCMT traverse strings of photographs of their facial veins.

The formation of veins on a person's face may additionally act as a means of distinguishing both twins who are identical and fraternal. We must undertake the development and testing of the novel methodology for the purpose of identifying situations involving identical twins. In order to enhance the accuracy of our suggested approach, we may integrate behavioral characteristics of an individual,

such as their gait signature, writing with a pen and gestures, together with the shape of their facial vessels.

Reference

[1]. Amirthavalli Kannika, and Kirubha D., "Thermal Imaging as a Biometrics Move Towards Facial Signature Substantiation", International Journals of Advanced Computational Engineering & Networking, Vol. 2, No. 1, pp.54-58, 2014.

[2]. Arandjelovic Ognjen, Hammoud B. Riad and Cipolla Robberto, "Thermal and Reflectance Based Personal Identification Methodology Under Variable Illumination", Pattern Recognition, Vol. 43, No. 5, pp. 1801-1813, 2010.

[3]. Buddharaju Pradeep, Pavlidis Loannis and Manohar Chinmay, "Face Recognition Beyond The Visible Spectrum", Advances in Biometrics, Springer London, pp. 157-180, 2008.

[4]. Chekmenev Sergey Y., Farag Aly A. and Essock Adward A., "Thermal Imaging of the Superficial Temporal Artery: An Arterial Plus Recovery Model" IEEE Conference on Computer Vision and Pattern Recognition, pp. 1-7, 2007.

[5]. Chen Cunjian, and Ross Arun, "Evaluation of Gender Classification Methods on Thermal and Near Infrared Face Image", Biometric International Conference, IEEE, pp. 1- 8, 2011.

[6]. Chennamma H. R., Rangarajan Lalitha, and Veerabhadrappa, "Face Identification From Manipulated Facial Images Using SIFT", IEEE International Conference on Emerging Trends in Engineering and Technology, pp. 192-195, 2010.

[7]. Cho Siu Yeung, Ting Chan Wai, and Quek Chai, "Thermal Facial Pattern Recognition for Personal Verification Using Fuzzy CMAC Model", International journal of innovative, Information and Control, Vol. 7, pp. 203-222, 2011.

[8]. Deepamalar M., and Madheswaram M., "An Improved Multimodal Palm Vein Recognition System Using Shape and Texture Features". International Journal of Computer Theory and Engineering, Vol. 2, pp. 95-101, 2010.

[9]. Garbey Marc, Sun Nanfei, Merla Arcangelo, and Pavlidis Loannis, "Contact-Free Measurement of Cardiac Plus Based on The Analysis of Thermal Imagery", Biomedical Engineering, IEEE, Vol. 54, pp. 1418-1426, 2007

[10]. Gault Travis R., Blumenthal Nicholas, FaragAly A., Starr Tom, "Extraction of the Superficial Vasculature, Vital Sign Waveform & Rates Using Thermal Imaging", Computer Vision and Pattern Recognition Workshops, IEE,pp. 1-8, 2010.

[11]. Ghiassa Reza Shoja, Arandjelovi Ognijen, Bendadaa Abdelhakim, and Maldague Xavier, "Infrared Face Recognition", Audio – Video Based Biometrics Person Authentication, Springer Berlin Heidelberg, Vol. 47, pp. 2807-2824, 2014.

[12]. Guzman Ana M., Goryawala Mohammmed, and Adjouadi Malek, "Generating Thermal Signatures Using Thermal Infrared Images", IEEE International Conference on Emerging Signal Processing Application, pp. 21-24, 2012.

[13]. Guzman Ana M. , Goryawala Mohammed, Wang Jin, Barreto Armando, Andrian Jean, Rishe Naphtali, and Adjouadi Malek, "Thermal Imaging as a Biometrics Approach to Facial Signature Authentication", Biomedical and Health Informatics, IEEE Journal, Vol. 17, pp.214- 222, 2013.

[14]. Hartung Daniel, Olsen Martin Aastrup, XuHaiyun, and Busch Christoph, "Spectral Minutiae for Vein Pattern Recognition", Biometrics International Joint Conference, IEEE, pp. 1-7, 2011.

[15]. Hartung Daniel, "Vascular Pattern Recognition and its Application in Privacy – Preserving Biometric Online – Banking System", Ph. D. dissertation, Gjovik University College, 2012.

[16]. Kumar MG Sanjith, and Saravanan D, "A Novel Approach To Face Recognition Based On Thermal Imaging", International Journal of Engineering Research and Technology, Vol.3, pp. 5-9, 2014.

[17]. KuratateTakaaki, Riley, Marcia, Pierce Brennand, Cheng Gordon, "Gender Identification Bias Induced with Texture Image on a Life Size Retro-Projected Face Screen", ROMAN, IEEE International Symposium on Robot and Human Interactive Communication, pp. 43-48,2012.

[18]. Lavanya A, Monika S, Sowmiya M., "Thermal Imaging and Facial Recognition Using Biometric Approach", IJESC Journal, Vol. 16, pp. 62-69, Jan 2014.

[19]. Martinez Brais, Binefa Xavier, and Pantic Maja, "Facial Component Detection in Thermal Imagery ", Computer and Pattern Recognition Workshops, IEEE, pp. 48-54, 2010.

[20]. Mekyska Jiri, Duro Virginia Espinosa, and Zanuy Marcos Faundez, "Face Segmentation: A comparison Between Visible and Thermal Image", IEEE International Carnahan Conference on Security Technology, pp.185-189, 2010.
[21]. Mishra Kamta Nath, Srivastava P. C., Agrawal Anupam, Garg Rishu and Singh Ankur, "Minutiae Fusion Based Framework for Thumbprint Identification of Identical Twins", International Journal of Intelligent Systems and Applications, Vol. 6, No. 1, pp. 84-101, 2014.
[22]. Mottl Vadim, Kopylov Andrey, Kostin Alexey, and Yermakov Alexey, "Elastic Transformation of the Image Pixel Grid for Similarity Based Face Identification", Pattern recognition, Proceedings, of IEEE International Conference, Vol. 3, pp. 549-552, 2002.
[23]. Negied Nermin K., "Moving Toward Thermal Imaging", International of Recent technology and Engineering, Vol. 2, pp. 73-77, 2014.
[24]. Nithyakalyani K., and Jayanthi T., "Face Recognition As A Biometrics Approach Using Thermal Images", International Journal of Advances in Science Engineering and Technology, Vol.2, pp. 93-98, 2014.
[25]. Osia Nnamdi, and Bourlai Thirimachos, "Holistic and Partial Face Recognition in the MWIR Band Using Manual and Automatic Detection of Face Based Features", Homeland Security, IEEE Conference on Technology, pp. 273-279, 2012.
[26]. Prakash K. N., Prasad K. Satya, "Color Local Binary Patterns for Image Indexing and Retrieval", International Journal of Intelligent Systems and Applications, vol.6, no.9, pp.68-74, 2014.
[27]. Seal Ayan, Ganguly Suranjan, Bhattacharjee Debotosh, Nasipuri Mita, Basu, and Dipak Kumar, "Minutiae Based Thermal Human Face Recognition Using Label Connected Component Algorithm", International Conference on Computer Communication, Control and Information Technology, Vol. 4, pp. 604-611, 2012.
[28]. Seal Ayan, Ganguly Suranjan, Bhattacharjee Debotosh, NasipuriMita, Basu, and Dipak Kumar, "Comparative Study of Human Thermal Face Recognition Based on Haar Wavelet Transformation(HWT) and Local Binary Pattern(LBP)", Computational Intelligence and Neuroscience , Vol. 17, pp.1-12, 2012 .
[29]. Seal Ayan, Bhattacharjee Debotosh, NasipuriMita, Basu, and Dipak Kumar, "Minutiae Based Thermal Face Recognition using Blood Perfusion Data", Procedia Technology, Vol. 3, pp. 604-611, 2013.
[30]. Seal Ayan, Ganguly Suranjan, Bhattacharjee Debotosh, Nasipuri Mita, Basu, and Dipak Kumar," Automated Thermal Face Recognition Based on Minutiae Extraction", ACM International Journal of Computational Intelligence Studies, Vol. 2, pp. 133-156, 2013 .
[31]. Shan Shiguang, Gao Wen, and Zhao Debin, "Face Identification From A Single Example Image Based on Face Specific Sub Space", Acoustics, Speech and Signal Processing, IEEE International Conference, Vol. 2, pp. II(21-25), 2002.
[32]. Srivastava P. C., Agrawal Anupam, Mishra Kamta Nath, Tripathi Vivek and Garg Rishu, "Fingerprints, Iris and DNA Features Based Multi-biometric Systems: A Review", International Journal of Information Technology and Computer Science, Vol. 5, No. 2, pp. 88-111, 2013.
[33]. Trujillo Leonardo, and Olague Gustavo, Hammoud Riad, Hernandez Benjamin, "Automatic Feature Localization in Thermal Images for Facial Expression Recognition", Computer Vision and Pattern Recognition Workshops, IEEE Computer Society Conference, Vol. 3, pp. 14-14, 2005.
[34]. Wang Ning, Li Qiong, A. Ahmed, Abd E1-Latif, Peng Jialing, NiuXiamu, "Multi-biometric Complex Fusion for Visible and Thermal Face Images", International Journal of Signal Processing, Image Processing and Pattern Recognition, Vol.6, pp. 1-16, 2013.
[35]. Wang Jian Gang, Sung Eric, "Facial Feature Extraction in an Infrared Image by Proxy with a Visible Face Image", Instrumentation and Measurement IEEE Transaction, Vol. 56, pp. 2057-2066, 2007.
[36]. Wong Wai Kit, Hui Joe How, "Face Detection in Thermal Imaging Using Head Curve Geometry", Image and Signal Processing IEEE International Congress, pp. 881-884, 2012.